© 2024 Journal of Pharmacy & Pharmacognosy Research, 12 (2), 264-285, 2024
ISSN 0719-4250
https://jppres.com

DOI: https://doi.org/10.56499/jppres23.1719_12.2.264

Original Article

Activity of propolis compounds as potential MMP1 and MMP2 inhibitors by *in silico* studies in wound healing application

[Actividad de compuestos de propóleos como inhibidores potenciales de MMP1 y MMP2 mediante estudios *in silico* sobre la cicatrización de heridas]

Adzani Gaisani Arda[1,2], Putri Hawa Syaifie[1*], Donny Ramadhan[1,3], Muhammad Miftah Jauhar[1,4], Dwi Wahyu Nugroho[1], Nofa Mardia Ningsih Kaswati[1], Alfian Noviyanto[1,5], Mega Safihtri[6], Nurul Taufiqu Rochman[7], Dimas Andrianto[6], Etik Mardliyati[8*]

[1]Nano Center Indonesia, Jl. Raya PUSPIPTEK, South Tangerang, Banten, 15314, Indonesia.
[2]Department of Biochemistry and Molecular Biology, Faculty of Medicine, University of Debrecen, Debrecen H-4032, Hungary.
[3]Research Center for Pharmaceutical Ingredients and Traditional Medicine, National Research and Innovation Agency (BRIN), Cibinong Science Center, West Java, 16911, Indonesia.
[4]Biomedical Engineering, Graduate School of Universitas Gadjah Mada, Sleman 55281, Yogyakarta, Indonesia.
[5]Department of Mechanical Engineering, Mercu Buana University, Jakarta 11650, Indonesia.
[6]Department of Biochemistry, Bogor Agricultural University, Jl. Raya Dramaga IPB Campus Dramaga Bogor, Bogor, 16680, Indonesia.
[7]Research Center for Advanced Material, National Research and Innovation Agency (BRIN), PUSPIPTEK, South Tangerang, Banten, 15314, Indonesia.
[8]Research Center for Vaccine and Drug, National Research and Innovation Agency (BRIN), Cibinong Science Center, West Java, 16911, Indonesia.
*E-mail: etik002@brin.go.id

Abstract

Context: Matrix metalloproteinases (MMPs) play a critical role in wound healing, with higher levels seen in chronic wounds, delaying healing. Since ancient times, propolis has been widely used for traditional wound healing. However, there is still limited research on MMP1 and MMP12.

Aims: To evaluate new candidates of propolis compounds for targeting MMP1 and MMP12 using *in silico* studies supported by experimental screening using LC-MS/MS quadrupole-time of flight (QTOF).

Methods: Compounds in propolis were screened using LC-MS/MS QTOF. The 3D structure of all compounds in propolis and protein targets was prepared in Autodock and Biovia Discovery Studio. The molecular docking of all compounds in propolis was carried out using Autodock on PyRx 0.9. Drug-likeness and ADMET analysis of selected compounds in propolis with the lowest affinity were observed. Lastly, molecular dynamic simulations of the best compounds in propolis were conducted using the GROMACS 2020 package.

Results: Eleven flavonoid and phenolic compounds were identified in propolis using LC-MS/MS QTOF analysis. Molecular docking simulations showed that licoflavone A and pinostrobin exhibited the lowest binding affinity to MMP1 and MMP12, respectively. Molecular dynamic simulations revealed that licoflavone A formed a more stabilized complex with MMP1, while pinostrobin formed a more stabilized complex with MMP12 than the native ligand.

Conclusions: This study revealed new candidates for MMP1 and MMP12 inhibitors from propolis compounds that can enhance wound healing. It is hoped that the evidence gathered in this study provides crucial new information in exploring new wound-healing medications.

Keywords: matrix metalloproteinases; molecular docking simulation; molecular dynamics simulation; propolis; wound healing.

Resumen

Contexto: Las metaloproteinasas de la matriz (MMP) desempeñan un papel fundamental en la cicatrización de las heridas, observándose niveles más elevados en las heridas crónicas, lo que retrasa la cicatrización. Desde la antigüedad, el propóleo se ha utilizado ampliamente para la cicatrización tradicional de heridas. Sin embargo, la investigación sobre las MMP1 y MMP12 sigue siendo limitada.

Objetivos: Evaluar nuevos candidatos de compuestos de propóleo para atacar MMP1 y MMP12 mediante estudios *in silico* apoyados por cribado experimental utilizando LC-MS/MS cuadrupolo-tiempo de vuelo (QTOF).

Métodos: Los compuestos del propóleo se analizaron mediante LC-MS/MS QTOF. La estructura 3D de todos los compuestos del propóleo y de las proteínas diana se preparó en Autodock y Biovia Discovery Studio. El acoplamiento molecular de todos los compuestos del propóleo se llevó a cabo utilizando Autodock en PyRx 0.9. Se observó la afinidad a fármacos y el análisis ADMET de los compuestos seleccionados en el propóleo con menor afinidad. Por último, se realizaron simulaciones de dinámica molecular de los mejores compuestos del propóleo con el paquete GROMACS 2020.

Resultados: Se identificaron once compuestos flavonoides y fenólicos en el propóleo mediante análisis LC-MS/MS QTOF. Las simulaciones de acoplamiento molecular mostraron que la licoflavona A y la pinostrobina presentaban la menor afinidad de unión con la MMP1 y la MMP12, respectivamente. Las simulaciones de dinámica molecular revelaron que la licoflavona A formaba un complejo más estabilizado con la MMP1, mientras que la pinostrobina formaba un complejo más estabilizado con la MMP12 que el ligando nativo.

Conclusiones: Este estudio reveló nuevos candidatos a inhibidores de MMP1 y MMP12 a partir de compuestos de propóleos que pueden mejorar la cicatrización de heridas. Se espera que las pruebas reunidas en este estudio aporten nueva información crucial para explorar nuevos medicamentos para la cicatrización de heridas.

Palabras Clave: cicatrización de heridas; metaloproteinasas de matriz; propóleo; simulación de acoplamiento molecular; simulación de dinámica molecular.

ARTICLE INFO
Received: June 6, 2023.
Accepted: November 7, 2023.
Available Online: December 23, 2023.

AUTHOR INFO
ORCID: 0000-0002-2674-6295 (AGA) 0000-0002-7020-8582 (DWN) 0000-0003-1929-8188 (NTR)
0000-0001-8566-7960 (PHS) 0000-0001-5559-3657 (NMNK) 0000-0003-0480-2388 (MS)
0000-0001-6556-3160 (DR) 0000-0002-6371-6765 (AN) 0000-0002-3621-9659 (EM)
0000-0002-5826-5904 (MMJ) 0000-0003-4406-5810 (DA)

INTRODUCTION

Skin, the body's largest organ, serves as the primary barrier protecting the body from potential assault by a foreign organism or toxic substances (Grice and Segre, 2011). Upon injury, a series of biochemical processes are initiated to repair the skin damage, known as wound healing. This process is differentiated into four main phases: hemostasis (minutes to hours after injury), inflammation, proliferation (4-21 days), and tissue remodeling (21 days – 1 year) (Reinke and Sorg, 2012). Any disruption in these phases can result in delayed wound healing and an increased potential for excessive scarring (Landén et al., 2016).

Matrix metalloproteinase (MMP), an endopeptidase, participates in all the phases of wound healing. During inflammation, MMPs remove all damaged proteins and temporary ECM. In the proliferation phase, MMPs degrade the capillary basement membrane to promote angiogenesis and cell migration. Meanwhile, in tissue remodeling, MMP activity was decreased and induced the release of growth factor for remodeling. In this case, tissue inhibitors of metalloproteinase (TIMPs) play critical roles in balancing MMP activities by binding to the specific site and preventing ECM breakdown excessively (Ayuk et al., 2016; Kandhwal et al., 2022). However, in some conditions, the imbalance of MMPs and TIMPs leads to a poor healing process. MMP1, a significant collagenase, is expressed at the wound site during angiogenesis. It degrades type 1 collagen as an essential component of the dermis after that re-epidermization and migration of keratinocytes happen in wound healing. MMP1 activity is only valid until the wound is closed, after which it is automatically turned off in the remodeling phase. However, a high level of MMP-1 was correlated with chronic wounds and led to prolonged healing time (Muller et al., 2008). For example, MMP1 drastically increased in diabetic foot ulcer patients. A ratio of MMP1/TIMP1 is used as a predictor of wound healing in diabetic foot ulcers. While more ratio MMP1 than TIMP1, the worse the healing. Previous studies have found that MMP levels are higher in chronic wound exudates than acute wound exudates (Lobmann et al., 2002). MMP12, a metalloelastase, also plays a significant role in wound healing. It destroys extracellular matrix elastin and allows immune cells responsible for inflammation and granuloma development to infiltrate. MMP12 is also reported to have an impact on mild inflammation in patients with type 1 diabetes mellitus. MMP12 has been linked to mild inflammation in patients with type 1 diabetes mellitus and shows a positive correlation with celiac disease in intestinal injuries among type 1 diabetes mellitus patients (Bister et al., 2005). Studies have indicated that MMP12 significantly decreases the wound-healing process after a specific plasma therapy was applied to 24 patients with chronic wounds (Ngoc Tuan et al., 2021). MMP1 and MMP12 may be MMP major targets in discovering new wound-healing candidate compounds.

Pharmaceutical studies regarding wound-healing compounds, particularly those derived from natural sources, are rapidly expanding. These sources contain polyphenol and flavonoid compounds with antioxidant activity that can inhibit skin deterioration enzymes. A previous study by Karakaya et al. (2020) showed the antioxidant and collagenase inhibition of *Epilobium angustifolium* extract. The bioactive compound of the extract also demonstrated wound-healing activity by inhibiting collagenase. In a medicinal plant *Plantago major* study, the extract and the compound calceorioside B exert significant inhibitory effects against collagenase (Genc et al., 2020).

Propolis, a resin collected by honeybees, contains high levels of antioxidants, approximately 20% of which are flavonoids. Several studies have reported its high antioxidant activity and various pharmacological effects such as anti-inflammation, antibacterial, anticancer, immunomodulatory, antiviral, anti-aging, antidiabetic, neuroprotective, anti-caries, and as a wound-healing agent (Campos et al., 2015; Fitria et al., 2021; Forma and Bryś, 2021; Iyyam Pillai et al., 2010; Jauhar et al., 2022; Kim et al., 2020; Pobiega et al., 2019; Syaifie et al., 2022a; 2022b; Touzani et al., 2019). Propolis ointment displays notable wound-healing activity in rats' skin and comparable activity with standard drugs (Iyyam Pillai et al., 2010). *In vitro* studies also observed wound-healing activity in human dermal fibroblasts (Afonso et al., 2020). Studies have also shown its inhibitory effects on collagenase and elastase activities, as Senol Deniz et al. (2021) reported. Another study conducted by Vilela et al. (2015) demonstrated the activity of caffeic acid phenethyl ester (CAPE) in reducing secreted protein levels of MMP1 and MMP9. A more recent focus in propolis-MMP interaction studies has centered on targeting MMP9. Immunohistochemistry on a skin wound model in male Wistar rats treated with Brazilian red propolis yielded decreased levels of MMP9 in the center and border areas of wounds within 14 days, along with improved wound healing and increased collagen (Conceição et al., 2022). In diabetic mice induced by streptozotocin, topical application of propolis improved the diabetic wound-healing process by lowering MMP9 and some inflammatory cytokines to normal levels (Hozzein et al., 2015). A report study also supports wound-healing enhancement of topical application propolis. In diabetic foot

ulcers, topical propolis application significantly decreases MMP9 levels with no adverse effects, leading to good wound closure (Henshaw et al., 2014). Besides, propolis studies on MMP1 and MMP12 in wound healing are still limited, and candidate compounds that strongly interact with MMP1 and MMP12 are still unclear. At the same time, MMP1 and MMP12 have a significant role in preventing prolonged wound healing.

This study aims to reveal new propolis compounds targeting MMP1 and MMP12 in wound healing. Active compounds of propolis were identified by LC-MS/MS quadrupole-time of flight (QTOF), followed by predicting their interactions with the targets through molecular docking and dynamic simulations. Drug-likeness and ADMET, properties of selected best compounds, were also analyzed. As a result, our studies discover new candidates of MMP1 and MMP12 inhibitors derived from propolis compounds to enhance wound healing. It is hoped that the evidence-gathering of this study provides important new information in exploring new wound-healing medications.

MATERIAL AND METHODS

Propolis screening (LC-MS/ MS QTOF)

The propolis, sourced from Apivent in Indonesia, was obtained in a brownish liquid extract form and harvested from *Apis mellifera* bees in East Asia since 2022. The analysis of the propolis extract involved a series of steps using liquid chromatography-mass spectrometry (LC-MS/MS). Initially, 1 mL of the extract was placed in a 10 mL volumetric flask with 9 mL of methanol and filtered through a 0.2 µm pore size PTFE syringe filter. Subsequently, 2 mL of the filtered solution was transferred to a 2 mL tube for the LC-MS/MS analysis. The LC-MS/MS analysis utilized an XEVO G2XS Quadrupole time-of-flight (Q-TOF) mass spectrometer manufactured by Waters in New Zealand. Separation was achieved using an Acquity UPLC HSST3 column (100 × 2.1 mm, 1.7 µm). The column temperature was maintained at 40˚C, and the sample temperature was maintained at 25˚C. The mobile phases included 0.1% formic acid in water (A) and 0.1% formic acid in acetonitrile (B). The flow rate was 0.6 mL/min, with an elution gradient from 1% A to 35% A in 16 min, followed by a linear gradient to 100% A over 2 min and a 2 min hold at 100% A. To screen the propolis compounds, a 2 µL test solution was injected, and the chromatographs were recorded for 20 min. The mass scan range during electrospray ionization (ESI) in positive ion mode was 50-1200 Da. The source and desolvation temperatures were set at 120˚C and 550˚C, respectively. The capillary and cone voltages were maintained at 2.0 kV and 40 V, respectively. The glass flow rates were set at 50 L/h for the cone and 1000 L/h for desolvation. Additionally, the low and high collision energies were 6 eV and 15-40 eV (ramp), respectively. For mass correction during acquisition, a leucine-enkephalin solution (1 ng/ml) was used as an external reference (lock spray). This lock spray was injected at 30 s, with a flow rate of 10 to 10 µL/min and a scan time of 0.1 s (Harisna et al., 2021).

Retrieval and preparation of protein structure for molecular docking

The 3D forms of MMP1 (PDB ID: 966C) and MMP12 (PDB ID: 1Y93) were obtained from the Protein Data Bank (http://www.rcsb.org). The crystal structure of the proteins involved removing the native ligand and water molecules. Through the utilization of Autodock 4.2 (Huey et al., 2012), non-polar hydrogens were combined, and polar hydrogens and Gasteiger charge were added.

Ligand preparation for molecular docking

The ligands extracted from the protein structure (native ligand) and the propolis compounds or the candidate ligands were utilized in docking simulations. Furthermore, reference compounds for each protein were also used in this study. The reference compounds were identified using the DrugBank database (https://go.drugbank.com/) by searching for drug compounds that target interstitial collagenase (MMP1) or macrophage metalloelastase (MMP12). We found marimastat as an MMP 1 inhibitor and acetohydroxamic acid as an MMP12 inhibitor (Belotti et al., 1999; Heath and Grochow, 2000; Mannino et al., 2006). Consequently, eleven compounds of propolis and two reference compounds (marimastat and acetohydroxamic acid) were retrieved in Structure Data Format (SDF) from the PubChem database (www.pubchem.ncbi.nlm.nih.gov). Ligands were prepared using Autodock 4.2 by merging non-polar hydrogen molecules, polar hydrogen molecules, and Gasteiger charges (Huey et al., 2012).

Molecular docking and docking validation

The grid position for molecular docking was determined by positioning the native ligand of each protein in the center of the ligand with the size of 40 × 40 × 40 Å using Autodock 4.2 (Huey et al., 2012). The grid box coordinates for MMP1 were X = 9.166, Y= -10.353., and Z = 38.398, while coordinate for MMP12 were X = 1.518, Y = -1.956, and Z = 4.736. Molecular docking analysis was performed using Autodock on PyRx 0.9 (https://pyrx.sourceforge.io/) (Dallakyan and Olson, 2015). Molecular docking studies use the

Lamarck Genetic Algorithm (LGA). In the docking validation method, the native ligand was re-docked with the protein to calculate the root mean square deviation (RMSD) with Autodock 4.2 compared to the original native ligand confirmation to the receptor (Huey et al., 2012). After validation steps achieved the criteria of RMSD less than 2, All propolis compounds and reference compounds were docked onto MMP1 and MMP12. Visualization of docking was done using Biovia Discovery Studio 2021. The ligand poses with the most favorable binding energy (-ΔG, kcal/mol) was chosen and used for further analysis. The interactions between H-bond, hydrophobic, charge, and van der Waals were also examined.

Drug-likeness and ADMET prediction

Absorption, distribution, metabolism, excretion, and toxicity describe pharmacokinetic profile properties of oral and dermal. In this study, ADMET properties and physicochemical parameters of drug-likeness descriptors like Lipinski's "rule of five" skin permeability (Log Kp) and skin sensitization of selected hit compounds and references compounds were evaluated using SwissAdme (http://www.swissadme.ch/) and pkCSM web server (http://biosig.unimelb.edu.au/pkcsm) (Daina et al., 2017; Pires et al., 2015). The data input was in SMILES format, retrieved from the PubChem database using DataWarrior software (Sander et al., 2015).

Molecular dynamics

Molecular dynamics (MD) simulations were performed using the GROMACS 2020 package to study the binding of two ligands and reference compounds to each of the four proteins. The ligands and proteins were in PDB format, and the protein topologies were generated using the Gromacs96 53A6 force field. The ligand topologies were generated using the PRODRG web server. A cubic box was created for the protein-ligand complex, and sodium and chloride ions were added to neutralize the charge. The system was minimized using the steepest descent algorithm for 5000 steps. The solvent and ions were equilibrated in two restrained phases at 300 K and 1.0 bar. Unrestrained MD simulations were then performed for 50 ns using the leapfrog integrator with a step size of 2 fs. The LINCS algorithm was used to constrain the covalent bonds, and the electrostatic interactions were calculated using the Particle Mesh Ewald (PME) method. The short-range van der Waals cut-off was set to 1.2 nm. Modified Brenden thermostat and Parrinello-Rahman barostat were used for temperature and pressure coupling, respectively. The root mean square deviation (RMSD), root mean square variation (RMSF), radius of gyration (Rg), and solvent accessible surface area (SASA) were calculated from the MD trajectories using the GROMACS integrated tool (Abraham et al., 2015; Essmann et al., 1995; Hess et al., 1997; Oostenbrink et al., 2004; van Aalten et al., 1996).

Data analysis

The data analysis was carried out in multiple steps: (1) propolis (Apivent) were screened for their bioactive compounds by using LC-MS/MS QTOF; (2) 3D structure of all propolis compounds and protein targets (MMP-1 and MMP-12) were prepared; (3) validation molecular docking was done by re-docking co-crystallized ligand of each target in optimal condition to ensure that docking method is reliable, then molecular docking of all propolis compounds carried out; (4) drug-likeness and ADMET analysis of selected propolis compounds that have lowest affinity from docking results were observed; (5) molecular dynamic simulation of best propolis compounds which have the best properties of binding affinities, drug-likeness and ADMET were carried out in 50 ns run; and (6) finally, this analysis aims to identify novel propolis compounds targeting MMP1 and MMP12.

RESULTS AND DISCUSSION

Bioactive compounds of propolis identified by LC-MS/MS QTOF

A total of 11 compounds of commercial propolis were successfully screened and identified based on the similarity percentage of their retention time (Rt) and molecular mass with the database from UNIFI software (Fig. S1). The isolated compounds were ferulic acid, 3,4-dimethoxy-cinnamic acid, genistin, penduletin, isorhamnetin, naringenin, pinostrobin, kaempferide, ombuin, quercetin-3,3'-dimethyl ether, and licoflavone A. The structures of these compounds, along with the Rt, can be seen in Table 1.

To validate the screening technique, samples were gathered over a broad collision energy spectrum, with a lower energy setting at 6 eV and a higher range from 15-40 eV to acquire precise mass information for fragment compounds. Subsequently, the experimental fragments obtained were cross-referenced with the accurate mass library using UNIFI software. Identified compounds were confirmed as precise candidate compounds by verifying specific fragments in each sample with mass accuracies greater than 5 ppm compared to spectral reference data in the library. This confirmation aids in reducing the number of similar candidate compounds, including isomers. In addition to mass accuracies, three other criteria were used to select accurate candidates through the screening method: MZ RMS match percentage, responses greater than 300, and more than one fragment match.

Table 1. Identified propolis compounds

Rt (min)	Response	Formula	Mass error (ppm)	m/z	Isotope Match MZ RMS (%)	MS/MS product ion	Identification	Group
7.66	3586	$C_{10}H_{10}O_4$	4	195.0648	7.79	177.0542, 89.0384	Ferulic acid	Phenolic acid
9.91	7742	$C_{11}H_{12}O_4$	3.76	209.0816	10.51	191.0710, 163.0760	3,4-Dimethoxycinnamic acid	Phenolic acid
10.86	8237	$C_{21}H_{20}O_{10}$	0.95	455.0938	9.36	271.0605, 103.0543	Genistin	Isoflavones
11.20	24.915	$C_{18}H_{16}O_7$	0.07	345.0969	10.44	301.0700	Penduletin	Flavanone
12.48	62446	$C_{16}H_{12}O_7$	3.88	317.0668	5.8	199.0742, 302.0410	Isorhamnetin	Metoxyflavonol
12.84	101768	$C_{15}H_{12}O_5$	3.94	273.0768	3.24	199.076, 227.0705, 255.0654	Naringenin	Flavanone
13.67	42577	$C_{16}H_{14}O_4$	-1.93	271.0960	4.09	168.0373, 167.0338	Pinostrobin	Flavonoid o-glycosides
14.34	117813	$C_{16}H_{12}O_6$	-0.51	301.0705	4.96	286.0481, 258.0530	Kaempferide	Methylated flavonol
14.61	164794	$C_{17}H_{14}O_7$	2.39	331.0825	4.98	316.0588, 301.0352	Ombuin	Dimethoxy flavone
14.78	175303	$C_{17}H_{14}O7$	2.39	331.0820	4.98	316.0584, 301.03478, 217.0500	Quercetin-3,3'-dimethyl ether	Dimethoxy flavone
16.45	13606	$C_{20}H_{18}O_4$	2.90	323.1291	10.79	285.07661, 255.0663	Licoflavone A	Flavones

This approach suggests that a screening method relying on precise mass data, comprehensive evaluation of isotopic patterns, accurate mass fragmentation collection, and compounds with high responses provide dependable information for detection (Pascali et al., 2018).

The compounds identified predominantly consisted of bioactive compounds, especially flavonoids, across diverse groups. Our analysis revealed that propolis samples contain two dimethoxyflavones, an isoflavone, a methoxyflavonol, two flavanones, a flavonoid o-glycoside, a methylated flavonol, and a flavone. The diversity of active compounds in propolis is influenced by the variety of source plants used by honeybees in the resin production for propolis. Major components like ferulic acid, genistin, and naringenin are commonly found in propolis (Bhargava et al., 2021; El-Guendouz et al., 2019; Rivera-Yañez et al., 2020).

3D structures of all ligands

Eleven propolis compounds and two reference compounds [marimastat and acetohydroxamic acid (HAE)] were visualized in their 3D structures from accessible PubChem database in .sdf formats and processed in Biovia discovery studio visualizer. While native ligands of MMP1 and MMP12 were identified as RS2 (n-hydroxy-2-[4-(4-phenoxy-benzenesulfonyl)-tetrahydro-pyran-4-yl]-acetamide) and HAE (acetohydroxamic acid), respectively. Moreover, marimastat is a reference drug for MMP1, and HAE acts as a reference drug for MMP12 and is also a native ligand for the protein. It has been ensured that native ligands bind to key active residues of each protein. 3D structures of all ligands can be seen in Fig. 1.

Molecular docking validation of MMP1 and MMP12

The native ligands of MMP1, RS2 (n-hydroxy-2-[4-(4-phenoxy-benzenesulfonyl)-tetrahydro-pyran-4-yl]-acetamide), MMP12, and HAE (acetohydroxamic acid) were docked into the binding site of MMP1 and MMP12 with grid box position defined using Autodock. The re-docked orientation was compared with the crystallized orientation, resulting in RMSD 1.836 Å (MMP1) and 1.874 Å (MMP12), where RMSD < 2 indicated that the docking protocol was reliable for the docking studies of propolis compounds against MMP1 and MMP12. Fig. 2 depicts the overlay of the native ligand conformation before and after docking validation.

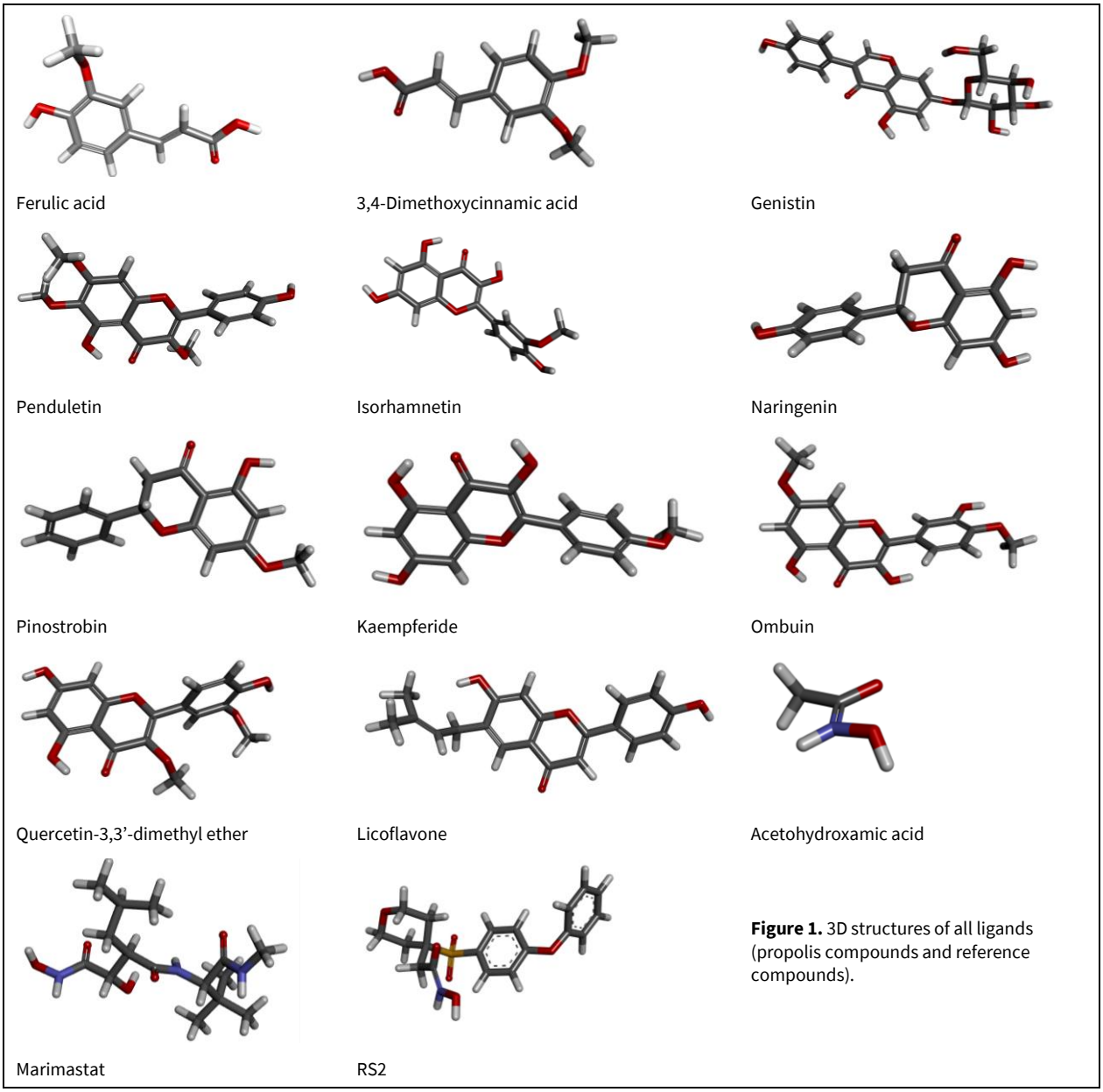

Figure 1. 3D structures of all ligands (propolis compounds and reference compounds).

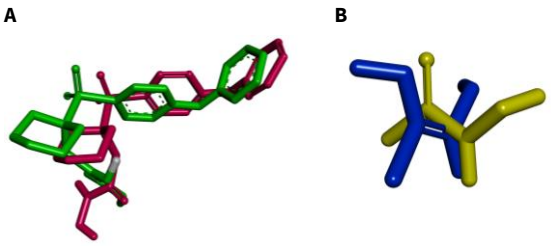

Figure 2. Overlay native ligand conformation MMP1 **(A)** before validation (green), after validation (pink), MMP12 **(B)** before validation (blue) after validation (yellow).

Molecular docking analysis of all ligands with MMP1 and MMP12

In analyzing the molecular docking results, the value of the free binding energy determined the best ligand. Binding free energy or binding affinity (ΔG) is the energy released because of bond formation or the interaction of protein and ligand, which modifies the energy of both the free receptor (protein) and the ligand. The binding energy directly affects the stability of the receptor-ligand complex, which is more stable when the free energy is negative. As a result, a negative value of (ΔG) is an essential property for an effective drug based on in silico study (De Vita et al., 2021).

Table 2. The predicted binding affinity of propolis and reference compounds against MMP1 and MMP12.

Compounds	Code	Binding affinity (Kcal/mol)	
		MMP1 (966C)	MMP12 (1Y93)
N-hydroxy-2-[4-(4-phenoxy-benzenesulfonyl)-tetrahydro-pyran-4-yl]-acetamide (native ligand)	RS2	-10.12	-
Marimastat (reference compound)	M	-5.94	-
Acetohydroxamic acid (native ligand and reference compound)	HAE	-	-3.82
Ferulic acid	P1	-5.17	-5.59
3,4-Dimethoxycinnamic acid	P2	-5.05	-5.58
Genistin	P3	-8.83	-6.22
Penduletin	P4	-7.67	-7.01
Isorhamnetin	P5	-8.45	-9.01
Naringenin	P6	-9.21	-8.73
Pinostrobin	P7	-8.39	-9.36
Kaempferide	P8	-8.58	-8.75
Ombuin	P9	-9.04	-7.27
Quercetin-3,3'-dimethyl ether	P10	-7.65	-7.3
Licoflavone A	P11	-10.03	-8.68

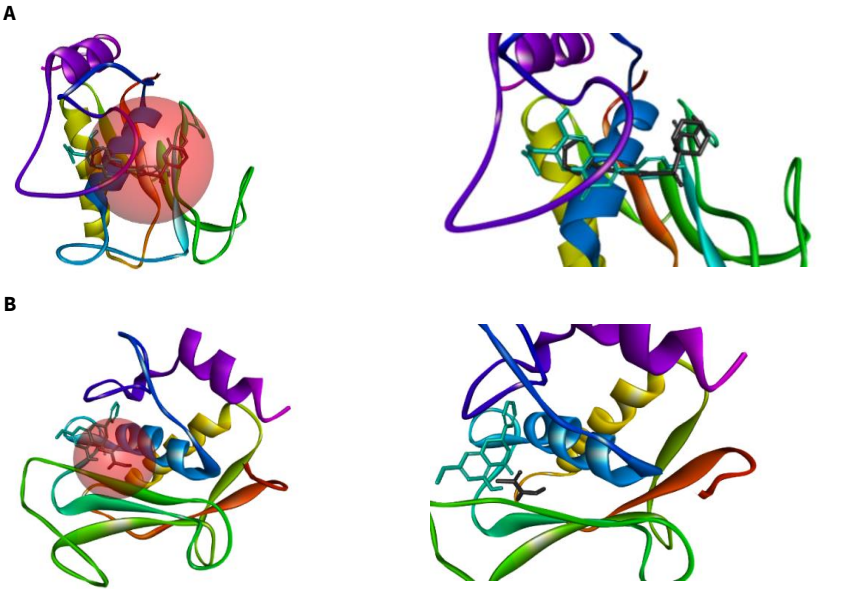

Figure 3. Binding orientation propolis compounds against MMP1 and MMP12 presented how they could be embedded in the same catalytic site of the receptor.

(A) Binding orientation with MMP1, RS2 = black, and licoflavone A (P8) = green. **(B)** Binding orientation with MMP12, HAE = black, and pinostrobin (P1) = green.

Eleven compounds found in propolis were successfully docked at MMP1 and MMP12 active sites. The docking score of propolis compounds against the two proteins is presented in Table 2. Among all compounds, licoflavone A (-10.03 kcal/mol) showed the lowest binding affinity to MMP1, and pinostrobin (-9.36 kcal/mol) showed the lowest binding affinity toward MMP12.

The interaction of the hit compound against MMP1 and MMP12 was presented in Fig. 3. The binding score of RS2 (native ligand) is slightly higher than propolis compound licoflavone A, which was -10.12

Kcal/mol, lower than all tested propolis compounds. However, all propolis compounds exhibit better binding scores to MMP1 than reference compounds, marimastat. Based on the binding affinity scores, the good binding affinity of propolis compounds against MMP1 was listed to licoflavone A (P11), naringenin (P6), ombuin (P9), genistin (P3), kaempferide (P8), isorhamnetin (P5), pinostrobin (P7), penduletin (P4), quercetin-3,3′-dimethyl ether (P10), ferulic acid (P1) 3,4-dimethoxycinnamic acid (P2). Table 3 depicts the interaction of propolis components at the active site with MMP1.

Licoflavone A demonstrates a higher binding affinity to MMP1 compared to all tested propolis compounds. It forms hydrogen bonds with ALA 182 (2.03 Å), ALA 234 (2.11 Å), and TYR 237 (3.03 Å), classifying these interactions as intermediate to robust hydrogen bonds. It also contacts six hydrophobic bonds with HIS 218, LEU 181, LEU 235, VAL 215, VAL 246, and TYR 240. The interactions between the hydrophobic side chain protein and the ligand significantly contribute to free energy binding. Water and other polar groups are repelled by hydrophobic moieties, resulting in the net attraction of non-polar ligand groups (Bronowska, 2011). The molecular interaction of MMP1 with the ligands is depicted in Fig. 4.

Meanwhile, in MMP12, all compounds found in propolis have higher scores than acetohydroxamic acid (HAE), as shown in Table 4. It suggests that the propolis compounds may exhibit superior inhibitory activity against elastase compared to acetohydroxamic acid.

As shown in Fig. 3, pinostrobin (P7) could be embedded in the same catalytic site of elastase with HAE. The exact position of the ligand and the protein can be seen in Fig. 5. Pinostrobin interacted with ALA 182 (3.00 Å) and TYR 240 (2.6 Å). A study by Elgamal et al. (2021) exhibits the potential of *Euphorbia retusa* against elastase. In this study, the compound quercetin-3-O-pentoside showed an excellent binding affinity toward MMP12 with hydrogen contacts to ALA182.

Table 3. The interaction of propolis compounds and reference compounds in the active site of MMP1.

Ligands	Binding energy (Kcal/mol)	Bond interaction	Amino acid residue
RS2	-10.12	Hydrogen	ALA 182, LEU 181, HIS 218, HIS 222, HIS 228
		Hydrophobic	VAL 215
		Ionic	HIS 218
		Van der Waals	ALA 184, ASN 180, ARG 214, GLU 219, LEU 235, HIS 183, PRO 238, SER 239, THR 241, TYR 237, TYR 240
Marimastat	-5.94	Hydrogen	GLY179, ALA182, GLU219, TYR210, TYR240
		Hydrophobic	VAL215, HIS218
		Ionic	-
		Van der Waals	LEU181
P11	-10.03	Hydrogen	ALA 182, ALA 234, TYR 237
		Hydrophobic	HIS 218, LEU 181, LEU 235, VAL 215, VAL 246, TYR 240
		Ionic	HIS 218
		Van der Waals	ARG 214, GLU 219, SER 239
P6	-9.21	Hydrogen	LEU 181, ALA 182, ALA 234
		Hydrophobic	VAL 215
		Ionic	HIS 218
		Van der Waals	ASN 180, ARG 214, GLU 219, LEU 235, MET 326, SER 239, TYR 240, PHE 242
P9	-9.04	Hydrogen	ASN 180, ALA 182, GLU 219, THR 241
		Carbon hydrogen	SER 239
		Hydrophobic	VAL 215
		Ionic	HIS 218
P3	-8.83	Hydrogen	GLY 179, ASN 180, ALA 182, SER 239

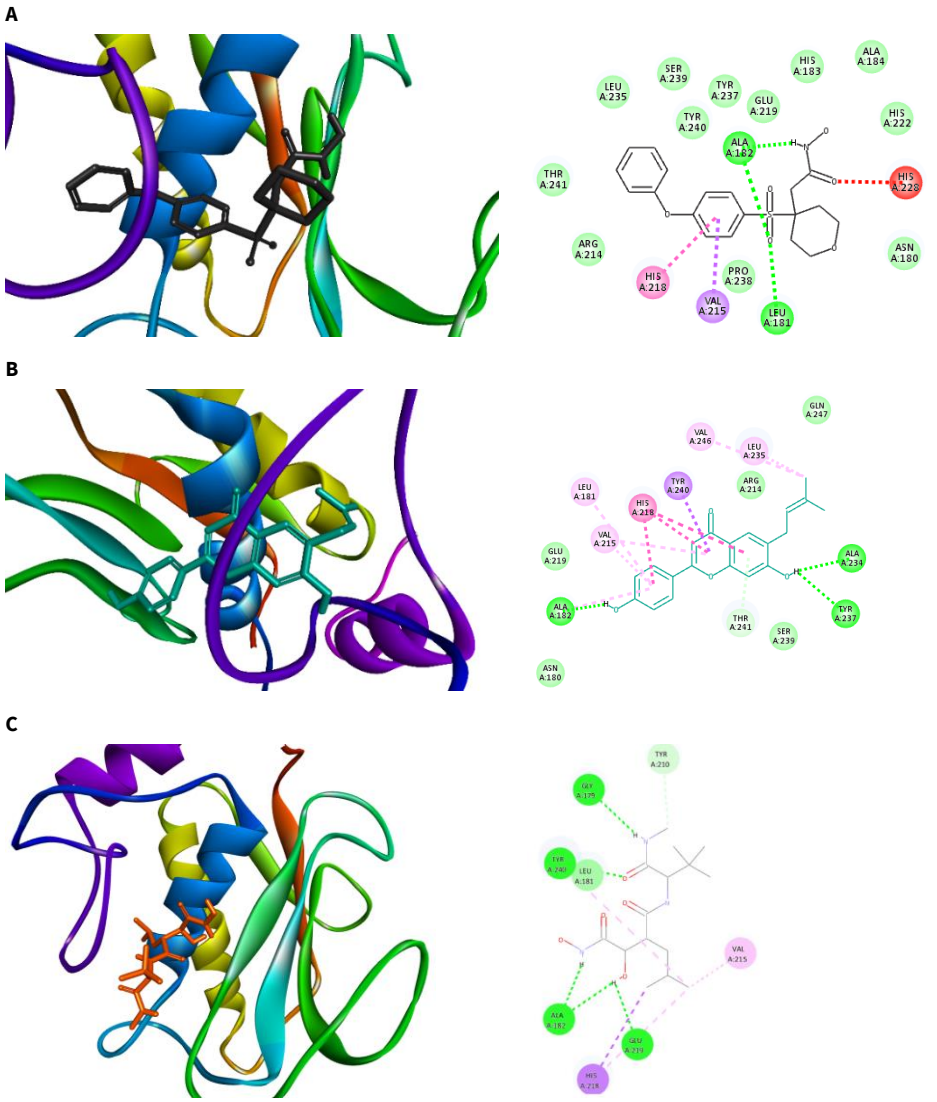

Figure 4. Molecular interaction of **(A)** RS2. **(B)** Licoflavone A. **(C)** Marimastat against MMP1.

Druglikeness and ADMET prediction of selected best propolis compounds

The two potential propolis compounds of each protein and its reference compounds were then evaluated for their ADMET physicochemical prediction using SwissADME and pKCSm (Table 5). None of these compounds violate the Lipinski rule, the essential criteria that a compound must meet to have drug-like properties. Compounds that meet the rule are more likely to be membrane-permeable and have a high bioavailability after oral administration, with a molecular weight of less than 500 g/mol, a Log P of less than 5, fewer than 5-H bond donors, fewer than 100 H-bond acceptors, and a molar refractivity of 40-130 (Lipinski et al., 1997). P11 showed a higher molecular weight than P7, and both values fell within an acceptable range. Skin permeability, assessed by LogKp values, remained within acceptable limits for all compounds. None of these compounds demonstrated skin-sensitizing potential upon toxicity analysis. Additionally, the reference compounds (marimastat and HAE) fulfilled nearly all drug-likeness and ADMET criteria, except for the MLogP parameter for HAE.

Molecular dynamics simulation of selected best propolis compounds

The MD simulation was run for 50 ns to investigate the stability and conformational changes of MMP1 and MMP12 structures when bound to the ligand. The root mean square deviation (RMSD), radius mean fluctuation (RMSF), radius of gyration (Rg), and solvent sccessible surface (SASA) were all calculated. RMSD is a plausible measure of protein stability. The RMSD data shows how far each frame deviated from the initial conformation of the reference structure as a function of time and is used to quantify differences between the structure sampled

Table 4. The interaction of propolis compounds in the active site of MMP12.

Ligands	Binding energy (Kcal/mol)	Bond interaction	Amino acid residue
HAE	-3.82	Hydrogen	ALA 182, HIS 222, HIS 228
		Van der Waals	GLU 219, HIS 218
P7	-9.36	Hydrogen	ALA 182, TYR 240
		Hydrophobic	ILE 180, LEU 181, HIS 218
		Van der Waals	LEU 214, GLU 219, THR 215, VAL 235
P5	-9.01	Hydrogen	GLY 179, ALA 182, GLU 219
		Carbon hydrogen	ALA 234, VAL 235, PHE 237
		Hydrophobic	ILE 180, LEU 181, HIS 218, TYR 240
		Ionic	HIS 218
		Van der Waals	LEU 214, GLU 219, THR 215, VAL 235
P8	-8.75	Hydrogen	ALA 182, GLU 219
		Carbon hydrogen	LEU 181, LEU 214
		Hydrophobic	ILE 180, LEU 181, VAL 235
		Ionic	HIS 218
		Van der Waals	GLY 179, VAL 217, THR 215, PHE 237, PRO 238, THR 239, LYS 241, PHE 248
P6	-8.73	Hydrogen	GLY 179, ALA 182, TYR 240
		Hydrophobic	ILE 180, HIS 218
		Van der Waals	LEU 214, THR 215, VAL 235, PHE 237, PRO 238, THR 239, LYS 241
P11	-8.56	Hydrogen	LEU 181, LEU 214
		Carbon hydrogen	ILE 180
		Hydrophobic	HIS 182, HIS 218, THR 239

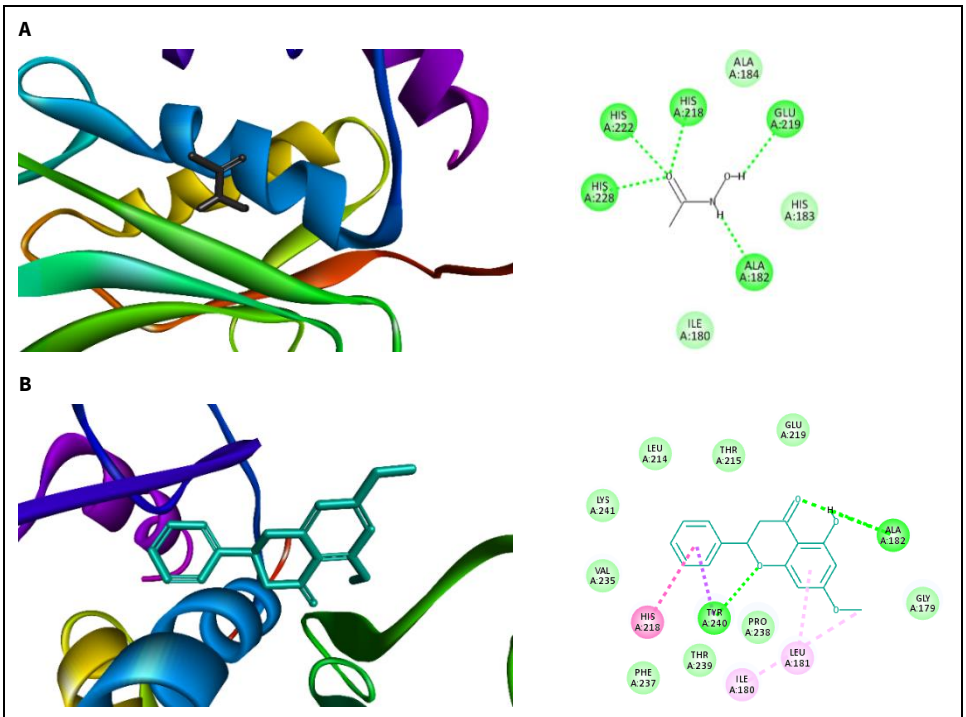

Figure 5. Molecular interaction of **(A)** HAE. **(B)** Pinostrobin against MMP12.

Table 5. Drug-likeness and ADMET prediction of four selected propolis compounds and reference compounds.

Variable	HAE	Marimastat	P11	P7
MW (g/mol)[a]	75.07	331.41	322.36	270.284
H-bond acceptors[b]	2	5	4	4
H-bond donors[c]	2	5	2	1
MLogP[d]	-0.96	0	1.67	1.52
Molar refractivity	15.46	84.86	97.63	74.02
RO5[f]	0	0	0	0
log Kp (cm/s)[g]	-4.134	-2.928	-2.739	-2.795
Skin sensitization[h]	NO	NO	NO	NO

[a]Molecular weight (acceptable range 130–500 gm/mol). [b]Acceptable H-bonds (acceptable range 0–10). [c]Donatable H-bonds (acceptable range 0–5). [d]MLogP (acceptable range 0–5). [e]Molar refractivity. [f]Rule of Five. [g]Skin permeant [acceptable range (− 8) - (− 1)]. [h]Predicted skin sensitization.

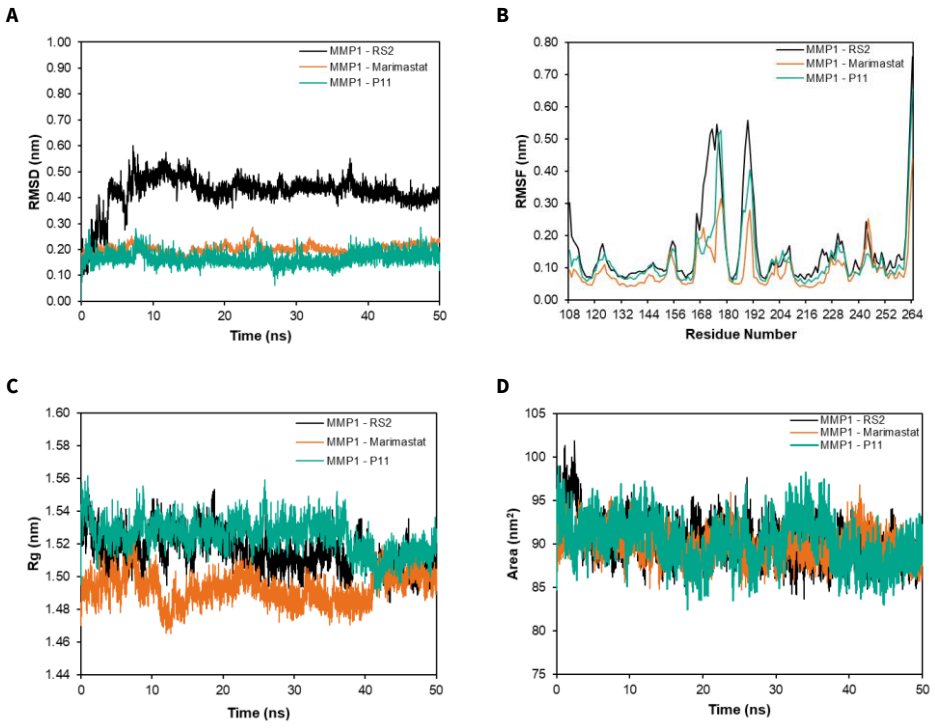

Figure 6. Molecular dynamic simulation trajectory analysis of MMP1-ligand complexes during 50 ns simulation.

(A) Backbone atoms' RMSD for MMP1-ligand complex. **(B)** Cα MMP1-ligand complex's RMSF. **(C)** MMP1-ligand complex's radius of gyration (Rg). **(D)** MMP1-ligand complex's SASA.

during the simulation and the reference structure (Martínez, 2015).

Fig. 6A showed that the system was equilibrated after approximately 10 ns for the MMP1-RS2 with an average RMSD value of 0.42 nm. Meanwhile, in the MMP1-marimastat complex and the MMP1-P11 complex, the system appears to be stable from 0 to 50 ns, with a slight fluctuation at 25-30 ns but remaining stable throughout the simulation with an average RMSD value of 0.20 and 0.17 nm, respectively.

RMSF quantifies the movement of a subset of atoms about the average structure throughout the simulation (Martínez, 2015). The fluctuations of the protein Cα atoms were measured to quantify the protein's flexibility in the presence of the ligand. Higher RMSF values indicate more significant changes in the residue. Fig. 6B depicts the RMSF of MMP1-RS2, MMP1-Marimastat, and MMP1-P11 complexes, with average RMSFs of 0.16, 0.09 and 0.13 nm, respectively. The RMSF plot revealed a significant fluctuation in the MMP1-RS2 complex around amino acids 173-176, 189,

and 264, indicating a change in conformation with RS2 binding. Meanwhile, MMP1-marimastat fluctuation at amino acids around 176-178, 188-189, and 263-264 appears to be lower than other complexes. The instability occurs around amino acid residues 177, 190, and 246, which fluctuate in the MMP1-P11 complex. According to the protein-ligand interaction mapping in the docking result (Table 2), the elevated amino acid did not bind directly to the ligand, indicating that it was not located in the protein's binding site. However, fluctuations decrease in most protein residues at positions 179-182, 215-218, 234-237, and 240-245, where amino acids directly bind to the protein via hydrogen, electrostatic, and hydrophobic bonds. The low RMSF value in binding site amino acids indicates that the residue forms a strong bond with the small molecule, resulting in optimal binding (Lobanov et al., 2008).

The radius of gyration was calculated to determine the structure's compactness. Over the simulation time, a stably folded protein maintains a reasonably constant Rg. According to Lobanov et al. (2008), a low Rg value indicates tight protein packing, whereas a high Rg value indicates looser protein packing. The changes in the Rg of protein MMP1 bonded to different ligands are shown in Fig. 6C. The nearly equal average Rg values of MMP1-RS2, MMP1-Marimastat, and MMP1-P11 are 1.52, 1.49 and 1.53 nm, respectively. The Rg of MMP1- RS2, MMP1-marimastat, and MMP1- P11 complex decline after 35 ns, signifies a compression in the protein structure.

SASA, or solvent-accessible access area, depicts changes in the protein's accessible surface area. It states how much a protein can interact with the solvent, and it is proportional to the degree to which a protein is exposed to the environment (Ali et al., 2014). In general, SASA corresponds to the molecular surface area that can be assessed by solvent molecules, providing a quantitative measure of the extent of protein/solvent (Pirolli et al., 2014). The result of the SASA analysis of MMP1 and the ligand analysis is reported in Fig. 6D. The same as the Rg, the average SASA value of the three proteins did not significantly differ from the value of 90 nm for both MMP1-RS2, MMP1-Marimastat, and MMP1-P11 complexes. As seen in the graph, these protein-ligand complexes slowly decrease at the end of the simulation. The decline can be attributed to protein structure compactness and the closing of water inlet valves of internal cavities, preventing water from diffusing into the protein's internal parts (Ebrahimi et al., 2021).

The RMSD of the backbone atoms of MMP12 with pinostrobin (P7) nearly stabilized at 0.40 nm from the start to the end of the simulation, as displayed in Fig. 7A. Meanwhile, the RMSD of the backbone atoms with HAE (native ligand) stabilized after 10 ns at 1.12 nm and slightly fluctuated. MMP12-HAE showed a greater average RMSD than MMP12-P7, which were 1.0 and 0.4 nm, respectively. The graph also depicts the stability of the MMP12-P7 complex over the MMP12-HAE complex. According to Kumari et al. (2020), the greater the RMSD value for one group or atom during the simulation, the greater the deviation from the initial position, resulting in more fluctuations in these values and greater protein structure instability. The RMSD diagram's slope and amplitude indicate the model's stability during simulation. The closer the slope is to zero, the lower the oscillation on the graph (Carugo and Pongor, 2001). Based on the graph and the average RMSD value, it may suggest that elastase binding to pinostrobin is more stable than protein binding to its native ligand.

In the RMSF, as depicted in Fig. 7B, the protein-ligand complex shows high fluctuation in the same residue. A significant difference is seen on residue 175, where MMP12-HAE fluctuates at 0.3 nm while the MMP12-P7 complex reaches 0.6 nm. ASP 175 is not a critical residue (Table 2); thus, this fluctuation did not affect the stability of protein-ligand binding. Moreover, the residues in the binding site located in positions 180-184, 218-219, 222, 228, and 240 had shown rigid behavior to HAE and hit the compound. In short, the RMSF plot indicates the structural stability of MMP12-ligand binding.

The radius of gyration value of the MMP12-ligand complex is illustrated in Fig. 7C. MMP12-HAE and MMP12-P7 have average Rg values of 1.51 and 1.50 nm, respectively. The Rg of the MMP12-HAE complex tends to fluctuate over time. MMP12-P7 has lower Rg values than MMP12-HAE. Low Rg values indicate that the molecules under investigation will remain stable and compact throughout the MD simulations. This parameter is defined as the mass-weighted RMSD of a group of atoms relative to their common mass center. Thus, structure stability is related to Rg tones reaching a plateau around the average values within a valid MD simulation (Likić et al., 2005). It has been demonstrated that MMP12 binding to propolis compound is more compact than binding to the native ligand.

MMP12-HAE and MMP12-P7 SASA trend to decrease over simulation. The reduced SASA tones indicate relative structural shrinkage for the protein/ligand due to solvent surface changes, resulting in more compact and stable conformations. The SASA was also calculated in the MMP12-ligand complex, as seen in Fig. 7D. The average values of the three complexes are 89.2, 87.7, and 88 nm^2. Based on the graph and the resulting value, these three complexes indicated compactness at the end of the simulation.

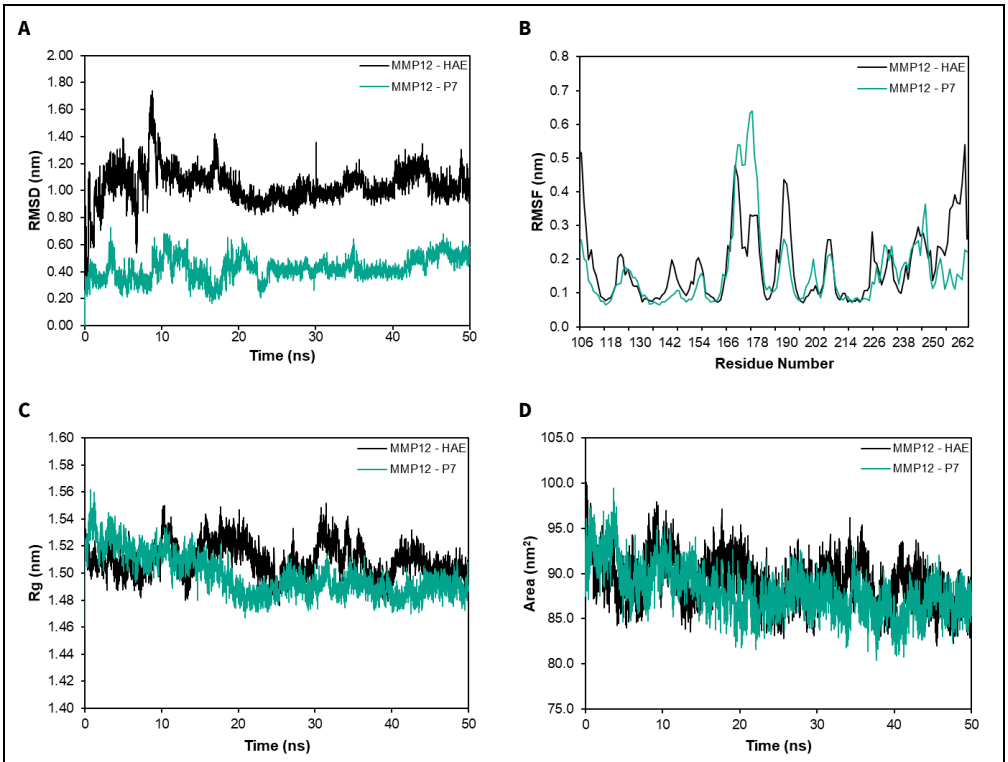

Figure 7. Molecular dynamics simulation trajectory analysis of elastase-ligand complexes during 50 ns simulation. Molecular dynamics simulations trajectory analysis of MMP12-ligand complexes during 50 ns simulation.

(A) Backbone atoms' RMSD for MMP12-ligand complex. **(B)** Cα MMP12-ligand complex's RMSF. **(C)** MMP12-ligand complex's radius of gyration (Rg). **(D)** MMP122-ligand complex's SASA.

Propolis, a resinous substance crafted from various plant components and chemicals released by bees, has been cherished for its therapeutic benefits since ancient times. It encompasses a broad spectrum of applications, offering antioxidant, antibacterial, antiviral, antitumor, immunomodulatory, anti-inflammatory, antidiabetic, anticancer, and wound healing properties. The pharmacological and medicinal potential of propolis largely hinges on its chemical composition and bioactive content. Propolis chemical compositions are intricately tied to the diversity of the surrounding flora, collection location, timing, and bee genetics (Santos et al., 2020; Scorza et al., 2020). Screening for all bioactive compounds in propolis is essential through a suitable method. Therefore, our study screened propolis using an advanced analytical technique and high-throughput analytical instruments, specifically LC-MS/MS QTOF.

LC-MS/MS QTOF was closely similar to the mass spectrometer triple quadrupole, with the third quadrupole replaced by time-of-flight. As an advanced quadrupole technology coupled with a mass spectrometer, each quadrupole has its crucial function in screening specific mass out of liquid chromatography separation. The first quadrupole acts as a mass filter, selecting specific ions based on their mass-to-charge ratio. The ions are then bombarded by neutral gas molecules like nitrogen or argon in the second quadrupole, resulting in ion fragmentation. This process is known as collision-induced dissociation (CID). After leaving the quadrupole, the ions are accelerated back to the ion modulator region of the time-of-flight analyzer, vibrating by the electric field and accelerated orthogonally to their original directions. All the ions that have acquired the same kinetic energy enter the flight tube, which is the field-free flow region where mass separation occurs. Ions that are lighter in mass will have a shorter flight time, while heavier ions will take longer to traverse the flight path to the detector (Ali et al., 2021; Wilschefski and Baxter, 2019). By using the mass library in UNIFI software, a batch of candidate compounds of propolis that matched with spectral data were elucidated and selected based on four criteria: (1) mass accuracies greater than 5 ppm, (2) response greater than 300, (3) more than 1 fragment match, (4) MZ RMS percentage lower than 11%. In results, this analytical method found eleven bioactive compounds in propolis that consist of a variety of flavonoid and phenolic groups, and they were ferulic acid, 3,4-dimethoxycinnamic acid, genistin, penduletin, isorhamnetin, naringenin, pinostrobin, kaempferide, ombuin, quercetin-3,3'-dimethyl ether, and licoflavone A (Table 1).

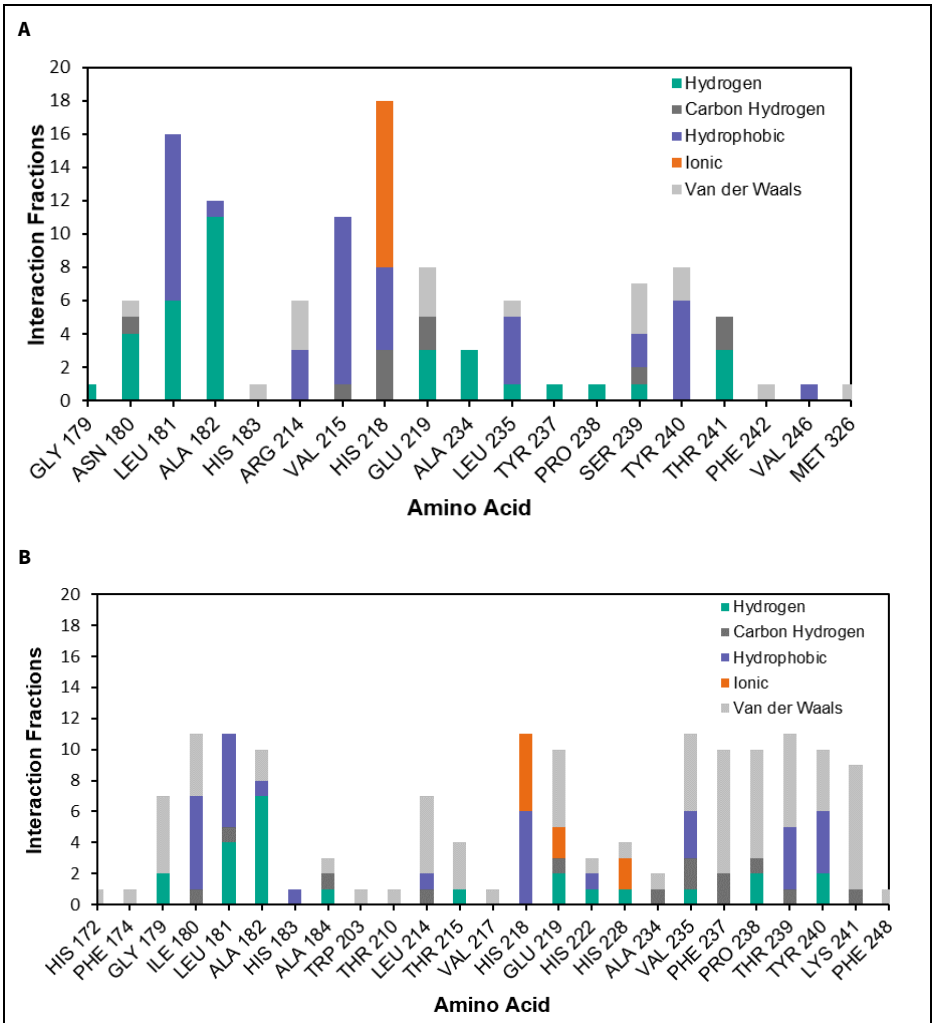

Figure 8. Amino acid residue interaction of top eleven propolis compounds against **(A)** MMP1 and **(B)** MMP12.

Propolis has been extensively studied for its wound-healing activity through multiple pharmacological mechanisms. Previous studies found that propolis has an antimicrobial agent to reduce biofilm formation, as it is an important factor in impaired wound healing. The antioxidant activity of propolis was utilized as a topical treatment for burn lesions. A severe burn is associated with the release of inflammatory mediators, including reactive oxygen species; thus, propolis may reduce severity by its antioxidant to prevent an inflammatory cascade. Propolis also has anti-inflammatory properties by obstructing nuclear factor *kappa* B, reactive oxygen species formation, and suppressing pro-inflammatory cytokines (Oryan et al., 2018; Rojczyk et al., 2020). In all phases of wound healing, endopeptidase matrix metalloproteinases (MMPs) have major roles in determining wound healing time. In some evidence, topical application of propolis effectively accelerates wound closure. Some studies have investigated the correlation of propolis and MMPS (Conceição et al., 2022; Henshaw et al., 2014).

There are 24 human MMPs that commonly form three categories: inactive, active, and complex MMPs. Their activities are regulated by tissue inhibitors of metalloproteinase (TIMPs) that are categorized into 4 types (TIMPs 1,2,3,4) (Kandhwal et al., 2022). During inflammation, MMPS removes all damaged proteins and temporary ECM. In the proliferation phase, MMPs degrade the capillary basement membrane to promote angiogenesis and cell migration. Meanwhile, in tissue remodeling, MMP activity was blocked by TIMPs and induced the release of growth factors for remodeling. Re-epithelialization is one of the most important parts of the healing process. However, in some injuries, the imbalance of MMPs and TIMPs leads to a poor healing process; for example, MMP1 drastically increases in diabetic foot ulcer patients and leads to prolonged healing time. High expression of MMP12 positively correlates with celiac disease in intestinal injury type 1 diabetes mellitus. Besides,

propolis studies on MMP1 and MMP12 in wound healing are still limited, and candidate compounds of propolis that strongly interact with MMP1 and MMP12 are still unclear (Caban et al., 2022; Leite, 2009; Ngoc Tuan et al., 2021; Quintero-Fabián et al., 2019; Wang and Khalil, 2018).

This study aims to reveal new candidates from propolis in targeting MMP1 and MMP12 for wound healing. Computational modeling is one technique that could aid in the fast screening and discovery of lead potential drugs at the lowest possible cost and time. Using molecular docking and molecular dynamic simulations makes the identification of lead candidates for *in vitro* and *in vivo* testing easier. Molecular docking identifies lead compounds with the highest binding affinity and best binding mode in virtual screening during the ligand-receptor simulation at the specific active site of a protein. However, molecular docking has limitations due to the lack of receptor flexibilities. Thus, this challenge can be met by using molecular dynamic (MD) simulation and also by determining the time-dependent dynamics of protein-ligand interactions. At the atomic level, MD simulation considers proteins, ligands, water molecules, and ions to be molecules interacting with one another via the integration of force fields derived from Newton's classical law of motion. Overall, MD simulation functions as a molecular microscope that can be used to inspect the stability of ligands in the active pocket of receptor targets, which is critical for validating the results predicted by the molecular docking-based virtual screening process (Adelusi et al., 2022; Glaab, 2016).

Molecular docking results of eleven propolis compounds to MMP1 and MMP12 were presented in Table 2. To better understand the mechanism of critical amino residue upon ten top compounds of propolis as MMP1 inhibitors, we fractionated the amino acid residue based on the interaction as shown in Fig. 8A. It was observed that HIS 218 was the most predominant among all amino acids, primarily interacting by forming ionic, hydrophobic, and carbon-hydrogen bonds. According to Leite et al., the HIS residue has a role in coordinating zinc ions in the active site. HIS 222 coordinates the zinc ion in the active site (Leite, 2009), while HIS 228 functions as a coordinator of the zinc within the catalytic site (Browner et al., 1995). The zinc ion was also coordinated by catalytic glutamate to bind the substrate (Cui et al., 2017). Thus, propolis compounds as inhibitors interact with the active site of MMP1 by chelating the catalytically active Zn^{2+}. As depicted in Fig. 8B, the HIS residue was frequently observed in the interaction of propolis compounds against macrophage metalloelastase (MMP12). This is because the zinc proteinase has a sequence like ALA-ALA-HIS-GLU, with aa-GLY-HIS being the molecular domain responsible for bonding to the zinc ion. In this domain, two histidine residues interact with the zinc ion (Leite, 2009). Arg 214 and Leucine in MMP1 and MMP12, respectively, form a shallow S1′ pocket (Laronha and Caldeira, 2020). This pocket is the most prominent because it determines the substrate specificity. It is also the most variable pocket in MMPs, where the cavity forms an Ω loop and is highly hydrophobic.

Based on binding affinities, binding modes, and key residue interactions, licoflavone A and pinostrobin exhibit the best potential candidates for targeting MMP1 and MMP12 among all tested propolis compounds. Licoflavone A and pinostrobin also possess drug-likeness and ADMET properties that meet the criteria for drug candidacy. To check the stability of binding these compounds to flexible modeled protein, molecular dynamic simulation runs in 50 ns for each ligand. Four parameters were represented in molecular dynamic results: RMSD, RMSF, radius gyration, and surface accessible solvent area (SASA). In comparison with the native ligand (RS21), licoflavone A showed a more stabilized complex with MMP1, as well as pinostrobin formed a more stabilized complex with MMP12 than the native ligand (HAE). Importantly, there were reduced fluctuations in the amino acid residues' position of binding site for licoflavone A to MMP1 compared to the native ligand (RS21). The affected residue positions were 179-182, 215-218, 234-237, and 240-245. Thus, the MD results showed a strong bond and optimal binding of licoflavone in the active site of MMP1. In the MD simulation of MMP12, pinostrobin also showed improved interactions and a more stabilized complex than the native ligand (HAE).

CONCLUSION

Eleven bioactive compounds, mainly comprising flavonoid groups, were positively identified in propolis by using LC-MS/MS QTOF. This study successfully used a computational screening strategy to find potential wound-healing agents in propolis by inhibiting collagenase (MMP1) and elastase (MMP12). Almost all eleven propolis compounds identified were considered potential candidate inhibitors of MMP1 and MMP12, with two compounds exhibiting the most favorable interactions with each protein, as indicated by in silico studies. Licoflavone A is a collagenase inhibitor, and pinostrobin is an elastase inhibitor, as demonstrated by molecular docking, ADMET prediction, and molecular dynamics simulation. The inhibitory activity of propolis compounds against MMP1 and MMP12 was revealed for the first time through an *in silico* study. Further, *in vitro* and *ex vivo*

testing of these compounds will be necessary to determine their wound-healing activity and asses their potential as agents for wound healing.

CONFLICT OF INTEREST

The authors declare no conflicts of interest.

ACKNOWLEDGMENTS

The authors express their gratitude to Apivent (PT Nano Herbaltama Internasional) for the propolis supply and computational facilities. The authors also thank Nano Center Indonesia for providing the facilities needed for this research. This research did not receive any specific grant from funding agencies in the public, commercial, or not-for-profit sectors.

REFERENCES

Abraham MJ, Murtola T, Schulz R, Páll S, Smith JC, Hess B, Lindahl E (2015) GROMACS: High performance molecular simulations through multi-level parallelism from laptops to supercomputers. SoftwareX 1–2: 19–25. https://doi.org/10.1016/j.softx.2015.06.001

Adelusi TI, Oyedele A-QK, Boyenle ID, Ogunlana AT, Adeyemi RO, Ukachi CD, Idris MO, Olaoba OT, Adedotun IO, Kolawole OE, Xiaoxing Y, Abdul-Hammed M (2022) Molecular modeling in drug discovery. Inform Med Unlocked 29: 100880. https://doi.org/10.1016/j.imu.2022.100880

Afonso AM, Gonçalves J, Luís Â, Gallardo E, Duarte AP (2020) Evaluation of the *in vitro* wound-healing activity and phytochemical characterization of propolis and honey. Appl Sci 10: 1845. https://doi.org/10.3390/app10051845

Ali A, Bashmil YM, Cottrell JJ, Suleria HAR, Dunshea FR (2021) LC-MS/MS-QTOF screening and identification of phenolic compounds from Australian grown herbs and their antioxidant potential. Antioxidants 10: 1770. https://doi.org/10.3390/antiox10111770

Ali S, Hassan Md, Islam A, Ahmad F (2014) A review of methods available to estimate solvent-accessible surface areas of soluble proteins in the folded and unfolded states. Curr Protein Pept Sci 15: 456–476. https://doi.org/10.2174/1389203715666140327114232

Ayuk SM, Abrahamse H, Houreld NN (2016) The role of matrix metalloproteinases in diabetic wound healing in relation to photobiomodulation. J Diabet Res 2016: 2897656. https://doi.org/10.1155/2016/2897656

Belotti D, Paganoni P, Giavazzi R (1999) MMP inhibitors: Experimental and clinical studies. Int J Biol Markers 14: 232–238. https://doi.org/10.1177/172460089901400406

Bhargava P, Mahanta D, Kaul A, Ishida Y, Terao K, Wadhwa R, Kaul SC (2021) Experimental Evidence for therapeutic potentials of propolis. Nutrients 13: 2528. https://doi.org/10.3390/nu13082528

Bister V, Kolho K-L, Karikoski R, Westerholm-Ormio M, Savilahti E, Saarialho-Kere U (2005) Metalloelastase (MMP-12) is upregulated in the gut of pediatric patients with potential celiac disease and in type 1 diabetes. Scand J Gastroenterol 40: 1413–1422. https://doi.org/10.1080/00365520510023918

Bronowska AK (2011) Thermodynamics of Ligand-Protein Interactions: Implications for Molecular Design. In Thermodynamics - Interaction Studies - Solids, Liquids and Gases. InTech. https://doi.org/10.5772/19447

Browner MF, Smith WW, Castelhano AL (1995) Crystal structures of matrilysin-inhibitor complexes. Biochemistry 34: 6602–6610. https://doi.org/10.1021/bi00020a004

Caban M, Owczarek K, Lewandowska U (2022) The role of metalloproteinases and their tissue inhibitors on ocular diseases: Focusing on potential mechanisms. Int J Mol Sci 23: 4256. https://doi.org/10.3390/ijms23084256

Campos JF, Santos UP dos, Rocha P dos S da, Damião MJ, Balestieri JBP, Cardoso CAL, Paredes-Gamero EJ, Estevinho LM, de Picoli Souza K, dos Santos EL (2015) Antimicrobial, antioxidant, anti-inflammatory, and cytotoxic activities of propolis from the stingless bee *Tetragonisca fiebrigi* (Jataí). Evid Based Complement Alternat Med 2015: 296186. https://doi.org/10.1155/2015/296186

Carugo O, Pongor S (2001) A normalized root-mean-spuare distance for comparing protein three-dimensional structures. Protein Sci 10: 1470–1473. https://doi.org/10.1110/ps.690101

Conceição M, Gushiken LFS, Aldana-Mejía JA, Tanimoto MH, Ferreira MVde S, Alves ACM, Miyashita MN, Bastos JK, Beserra FP, Pellizzon CH (2022) Histological, immunohistochemical and antioxidant analysis of skin wound healing influenced by the topical application of Brazilian red propolis. Antioxidants 11: 2188. https://doi.org/10.3390/antiox11112188

Cui N, Hu M, Khalil RA (2017) Biochemical and Biological Attributes of Matrix Metalloproteinases. In: Progress in Molecular Biology and Translational Science, 147: 1–73). https://doi.org/10.1016/bs.pmbts.2017.02.005

Daina A, Michielin O, Zoete V (2017) SwissADME: A free web tool to evaluate pharmacokinetics, drug-likeness and medicinal chemistry friendliness of small molecules. Sci Rep 7: 42717. https://doi.org/10.1038/srep42717

Dallakyan S, Olson AJ (2015) Small-molecule library screening by docking with PyRx. In: Hempel J, Williams C, Hong C (eds) Chemical Biology. Methods in Molecular Biology. New York, NY: Humana Press, vol. 1263: 243–250. https://doi.org/10.1007/978-1-4939-2269-7_19

De Vita S, Chini MG, Bifulco G, Lauro G (2021) Insights into the ligand binding to bromodomain-containing protein 9 (BRD9): A Guide to the selection of potential binders by computational methods. Molecules 26: 7192. https://doi.org/10.3390/molecules26237192

Ebrahimi KS, Ansari M, Hosseyni Moghaddam MS, Ebrahimi Z, Salehi Z, Shahlaei M, Moradi S (2021) *In silico* investigation on the inhibitory effect of fungal secondary metabolites on RNA dependent RNA polymerase of SARS-CoV-II: A docking and molecular dynamic simulation study. Comp Biol Med 135: 104613. https://doi.org/10.1016/j.compbiomed.2021.104613

Elgamal AM, El Raey MA, Gaara A, Abdelfattah MAO, Sobeh M (2021) Phytochemical profiling and anti-aging activities of *Euphorbia retusa* extract: *In silico* and *in vitro* studies. Arab J Chem 14: 103159. https://doi.org/10.1016/j.arabjc.2021.103159

El-Guendouz S, Lyoussi B, Miguel MG (2019) Insight on propolis from Mediterranean countries: Chemical composition, biological activities and application fields. Chem Biodivers 16: e1900094. https://doi.org/10.1002/cbdv.201900094

Essmann U, Perera L, Berkowitz ML, Darden T, Lee H, Pedersen LG (1995) A smooth particle mesh Ewald method. J Chem Phys 103: 8577–8593. https://doi.org/10.1063/1.470117

Fitria A, Hanifah S, Chabib L, Uno AM, Munawwarah H, Atsil N, Pohara HA, Weuanggi DA, Syukri Y (2021) Design and characterization of propolis extract loaded self-nano emulsifying drug delivery system as immunostimulant. Saudi Pharm J 29: 625–634. https://doi.org/10.1016/j.jsps.2021.04.024

Forma E, Bryś M (2021) Anticancer activity of propolis and its compounds. Nutrients 13: 2594. https://doi.org/10.3390/nu13082594

Genc Y, Dereli FTG, Saracoglu I, Akkol EK (2020) The inhibitory effects of isolated constituents from *Plantago major* subsp. major L. on collagenase, elastase and hyaluronidase enzymes: Potential wound healer. Saudi Pharm J 28: 101–106. https://doi.org/10.1016/j.jsps.2019.11.011

Glaab E (2016) Building a virtual ligand screening pipeline using free software: A survey. Brief Bioinform 17: 352–366. https://doi.org/10.1093/bib/bbv037

Grice EA, Segre JA (2011) The skin microbiome. Nat Rev Microbiol 9: 244–253. https://doi.org/10.1038/nrmicro2537

Harisna AH, Nurdiansyah R, Syaifie PH, Nugroho DW, Saputro KE, Firdayani Prakoso CD, Rochman NT, Maulana NN, Noviyanto A, Mardliyati E (2021) *In silico* investigation of potential inhibitors to main protease and spike protein of SARS-CoV-2 in propolis. Biochem Biophys Rep 26: 100969. https://doi.org/10.1016/j.bbrep.2021.100969

Heath EI, Grochow LB (2000) Clinical potential of matrix metalloprotease inhibitors in cancer therapy. Drugs 59: 1043–1055. https://doi.org/10.2165/00003495-200059050-00002

Henshaw FR, Bolton T, Nube V, Hood A, Veldhoen D, Pfrunder L, McKew GL, Macleod C, McLennan SV, Twigg SM (2014) Topical application of the bee hive protectant propolis is well tolerated and improves human diabetic foot ulcer healing in a prospective feasibility study. J Diabetes Complicat 28: 850–857. https://doi.org/10.1016/j.jdiacomp.2014.07.012

Hess B, Bekker H, Berendsen HJC, Fraaije JGEM (1997) LINCS: A linear constraint solver for molecular simulations. J Comput Chem 18: 1463–1472. https://doi.org/10.1002/(SICI)1096-987X(199709)18:12%3C1463::AID-JCC4%3E3.0.CO;2-H

Hozzein WN, Badr G, Al Ghamdi AA, Sayed A, Al-Waili NS, Garraud O (2015) Topical application of propolis enhances cutaneous wound healing by promoting TGF-beta/Smad-mediated collagen production in a streptozotocin-induced type I diabetic mouse model. Cell Physiol Biochem 37: 940–954. https://doi.org/10.1159/000430221

Huey R, Morris GM, Forli S (2012) Using AutoDock 4 and AutoDock Vina with AutoDockTools: A Tutorial. http://autodock.scripps.edu

Iyyam Pillai S, Palsamy P, Subramanian S, Kandaswamy M (2010) Wound healing properties of Indian propolis studied on excision wound-induced rats. Pharm Biol 48: 1198–1206. https://doi.org/10.3109/13880200903578754

Jauhar MM, Syaifie PH, Arda AG, Ramadhan D, Nugroho DW, Ningsih Kaswati NM, Noviyanto A, Rochman NT, Mardliyati E (2022) Evaluation of propolis activity as sucrose-dependent and sucrose-independent *Streptococcus mutans* inhibitors to treat dental caries using an *in silico* approach. J Appl Pharm Sci 13: 71–80. https://doi.org/10.7324/japs.2023.45365

Kandhwal M, Behl T, Singh S, Sharma N, Arora S, Bhatia S, Al-Harrasi A, Sachdeva M, Bungau S (2022) Role of matrix metalloproteinase in wound healing. Am J Transl Res 14: 4391–4405. http://www.ncbi.nlm.nih.gov/pmc/articles/pmc9360851/

Karakaya S, Süntar I, Yakinci OF, Sytar O, Ceribasi S, Dursunoglu B, Ozbek H, Guvenalp Z (2020) *In vivo* bioactivity assessment on *Epilobium species*: A particular focus on *Epilobium angustifolium* and its components on enzymes connected with the healing process. J Ethnopharmacol 262: 113207. https://doi.org/10.1016/j.jep.2020.113207

Kim DH, Auh J-H, Oh J, Hong S, Choi S, Shin EJ, Woo SO, Lim T-G, Byun S (2020) Propolis suppresses UV-induced photoaging in human skin through directly targeting phosphoinositide 3-kinase. Nutrients 12: 3790. https://doi.org/10.3390/nu12123790

Kumari P, Kumari M, Kashyap HK (2020) How pure and hydrated reline deep eutectic solvents affect the conformation and stability of lysozyme: Insights from atomistic molecular dynamics simulations. J Phys Chem B 124: 11919–11927. https://doi.org/10.1021/acs.jpcb.0c09873

Landén NX, Li D, Ståhle M (2016) Transition from inflammation to proliferation: A critical step during wound healing. Cell Mol Life Sci 73: 3861–3885. https://doi.org/10.1007/s00018-016-2268-0

Laronha H, Caldeira J (2020) Structure and function of human matrix metalloproteinases. Cell 9: 1076. https://doi.org/10.3390/cells9051076

Leite SRdeA (2009) Inhibitors of human collagenase, MMP1. Eclet Quim 34: 87–102. https://doi.org/10.1590/S0100-46702009000400008

Likić VA, Gooley PR, Speed TP, Strehler EE (2005) A statistical approach to the interpretation of molecular dynamics simulations of calmodulin equilibrium dynamics. Prot Sci 14: 2955–2963. https://doi.org/10.1110/ps.051681605

Lipinski CA, Lombardo F, Dominy BW, Feeney PJ (1997) Experimental and computational approaches to estimate solubility and permeability in drug discovery and development settings. Adv Drug Deliv Rev 23: 3–25. https://doi.org/10.1016/s0169-409x(00)00129-0

Lobanov MY, Bogatyreva NS, Galzitskaya OV (2008) Radius of gyration as an indicator of protein structure compactness. Mol Biol 42: 623–628. https://doi.org/10.1134/S0026893308040195

Lobmann R, Ambrosch A, Schultz G, Waldmann K, Schiweck S, Lehnert H (2002) Expression of matrix-metalloproteinases and their inhibitors in the wounds of diabetic and non-diabetic patients. Diabetologia 45: 1011–1016. https://doi.org/10.1007/s00125-002-0868-8

Mannino C, Nievo M, Machetti F, Papakyriakou A, Calderone V, Fragai M, Guarna A (2006) Synthesis of bicyclic molecular scaffolds (BTAa): An investigation towards new selective MMP-12 inhibitors. Bioorg Med Chem 14: 7392–7403. https://doi.org/10.1016/j.bmc.2006.07.028

Martínez L (2015) Automatic identification of mobile and rigid substructures in molecular dynamics simulations and fractional structural fluctuation analysis. PLoS One 10: e0119264. https://doi.org/10.1371/journal.pone.0119264

Muller M, Trocme C, Lardy B, Morel F, Halimi S, Benhamou PY (2008) Matrix metalloproteinases and diabetic foot ulcers: the ratio of MMP-1 to TIMP-1 is a predictor of wound healing. Diabet Med 25: 419–426. https://doi.org/10.1111/j.1464-5491.2008.02414.x

Ngoc Tuan N, Tran Ngoc Tu N, Tien Dung N (2021) Autologous platelet - rich plasma (PRP) therapy and changements of topical biological markers (EGF, VEGF and MMP12) of chronic wounds. Vietnam Med J 506: 32–44. https://doi.org/10.51298/vmj.v506i1-2.973

Oostenbrink C, Villa A, Mark AE, Van Gunsteren WF (2004) A biomolecular force field based on the free enthalpy of hydration and solvation: The GROMOS force-field parameter sets 53A5 and 53A6. J Comput Chem 25: 1656–1676. https://doi.org/10.1002/jcc.20090

Oryan A, Alemzadeh E, Moshiri A (2018) Potential role of propolis in wound healing: Biological properties and therapeutic activities. Biomed Pharmacother 98: 469–483. https://doi.org/10.1016/j.biopha.2017.12.069

Pascali JP, Fais P, Vaiano F, Bertol E (2018) Application of HRAM screening and LC–MS/MS confirmation of active pharmaceutical ingredient in "natural" herbal supplements.

Forensic Sci Int 286: e28–e31. https://doi.org/10.1016/j.forsciint.2018.03.014

Pires DEV, Blundell TL, Ascher DB (2015) pkCSM: Predicting small-molecule pharmacokinetic and toxicity properties using graph-based signatures. J Med Chem 58: 4066–4072. https://doi.org/10.1021/acs.jmedchem.5b00104

Pirolli D, Sciandra F, Bozzi M, Giardina B, Brancaccio A, De Rosa MC (2014) Insights from molecular dynamics simulations: Structural basis for the V567D mutation-induced instability of zebrafish alpha-dystroglycan and comparison with the murine model. PLoS One 9: e103866. https://doi.org/10.1371/journal.pone.0103866

Pobiega K, Kraśniewska K, Derewiaka D, Gniewosz M (2019) Comparison of the antimicrobial activity of propolis extracts obtained by means of various extraction methods. J Food Sci Technol 56: 5386–5395. https://doi.org/10.1007/s13197-019-04009-9

Quintero-Fabián S, Arreola R, Becerril-Villanueva E, Torres-Romero JC, Arana-Argáez V, Lara-Riegos J, Ramírez-Camacho MA, Alvarez-Sánchez ME (2019) Role of matrix metalloproteinases in angiogenesis and cancer. Front Oncol 9: 1370. https://doi.org/10.3389/fonc.2019.01370

Reinke JM, Sorg H (2012) Wound repair and regeneration. Eur Surg Res 49: 35–43. https://doi.org/10.1159/000339613

Rivera-Yañez N, Rivera-Yañez CR, Pozo-Molina G, Méndez-Catalá CF, Méndez-Cruz AR, Nieto-Yañez O (2020) Biomedical properties of propolis on diverse chronic diseases and its potential applications and health benefits. Nutrients 13: 78. https://doi.org/10.3390/nu13010078

Rojczyk E, Klama-Baryła A, Łabuś W, Wilemska-Kucharzewska K, Kucharzewski M (2020) Historical and modern research on propolis and its application in wound healing and other fields of medicine and contributions by Polish studies. J Ethnopharmacol 262: 113159. https://doi.org/10.1016/j.jep.2020.113159

Sander T, Freyss J, von Korff M, Rufener C (2015) DataWarrior: An open-source program for chemistry aware data visualization and analysis. J Chem Inf Model 55: 460–473. https://doi.org/10.1021/ci500588j

Santos LM, Fonseca MS, Sokolonski AR, Deegan KR, Araújo RPC, Umsza-Guez MA, Barbosa JDV, Portela RD, Machado BAS (2020) Propolis: types, composition, biological activities, and veterinary product patent prospecting. J Sci Food Agric 100: 1369–1382. https://doi.org/10.1002/jsfa.10024

Scorza CA, Gonçalves VC, Scorza FA, Fiorini AC, de Almeida A-CG, Fonseca MCM, Finsterer J (2020) Propolis and coronavirus disease 2019 (COVID-19): Lessons from nature. Complement Ther Clin Pract 41: 101227. https://doi.org/10.1016/j.ctcp.2020.101227

Senol Deniz FS, Orhan IE, Duman H (2021) Profiling cosmeceutical effects of various herbal extracts through elastase, collagenase, tyrosinase inhibitory and antioxidant assays. Phytochem Lett 45: 171–183. https://doi.org/10.1016/j.phytol.2021.08.019

Syaifie PH, Harisna AH, Nasution MAF, Arda AG, Nugroho DW, Jauhar MM, Mardliyati E, Maulana NN, Rochman NT, Noviyanto A, Banegas-Luna AJ, Pérez-Sánchez H (2022a) Computational study of Asian propolis compounds as potential anti-type 2 diabetes mellitus agents by using inverse virtual screening with the DIA-DB Web Server, Tanimoto similarity analysis, and molecular dynamic simulation. Molecules 27: 3972. https://doi.org/10.3390/molecules27133972

Syaifie PH, Hemasita AW, Nugroho DW, Mardliyati E, Anshori I (2022b) *In silico* investigation of propolis compounds as potential neuroprotective agent. Biointerface Res Appl Chem 12: 8285–8306. https://doi.org/10.33263/BRIAC126.82858306

Touzani S, Embaslat W, Imtara H, Kmail A, Kadan S, Zaid H, ElArabi I, Badiaa L, Saad B (2019) *In vitro* evaluation of the potential use of propolis as a multitarget therapeutic product: Physicochemical properties, chemical composition, and immunomodulatory, antibacterial, and anticancer properties. BioMed Res Int 2019: 4836378. https://doi.org/10.1155/2019/4836378

van Aalten DMF, Bywater R, Findlay JBC, Hendlich M, Hooft RWW, Vriend G (1996) PRODRG, a program for generating molecular topologies and unique molecular descriptors from coordinates of small molecules. J Comput Aided Mol Des 10: 255–262. https://doi.org/10.1007/BF00355047

Vilela PdGF, de Oliveira JR, de Barros PP, Leão MVP, de Oliveira LD, Jorge AOC (2015) *In vitro* effect of caffeic acid phenethyl ester on matrix metalloproteinases (MMP-1 and MMP-9) and their inhibitor (TIMP-1) in lipopolysaccharide-activated human monocytes. Arch Oral Biol 60: 1196–1202. https://doi.org/10.1016/j.archoralbio.2015.04.009

Wang X, Khalil RA (2018) Matrix metalloproteinases, vascular remodeling, and vascular disease. Adv Pharmacol 81: 241–330. https://doi.org/10.1016/bs.apha.2017.08.002

Wilschefski SC, Baxter MR (2019) Inductively coupled plasma mass spectrometry: Introduction to analytical aspects. Clin Biochem Rev 40: 115–133.

AUTHOR CONTRIBUTION:

Contribution	Arda GA	Syaifie PH	Ramadhan D	Jauhar MM	Nugroho DW	Kaswati NMN	Noviyanto A	Andrianto D	Rochman NT	Safithri M	Mardliyati E
Concepts or ideas	x	x		x			x	x	x	x	x
Design	x	x		x	x		x	x		x	x
Definition of intellectual content	x	x					x		x		x
Literature search	x	x									
Experimental studies		x				x					
Data acquisition	x		x		x					x	x
Data analysis	x	x	x	x	x	x					
Statistical analysis											
Manuscript preparation	x	x									x
Manuscript editing	x	x	x	x			x				x
Manuscript review	x	x	x	x	x	x	x	x	x	x	x

Citation Format: Arda GA, Syaifie PH, Ramadhan D, Jauhar MM, Nugroho DW, Kaswati NMN, Noviyanto A, Andrianto D, Rochman NT, Safithri M, Mardliyati E (2024) Activity of propolis compounds as potential MMP1 and MMP2 inhibitors by *in silico* studies in wound healing application. J Pharm Pharmacogn Res 12(2): 264–285. https://doi.org/10.56499/jppres23.1719_12.2.264

Supplementary data

Ferulic acid (4-Hydroxy-3-methoxy-cinnamic acid)

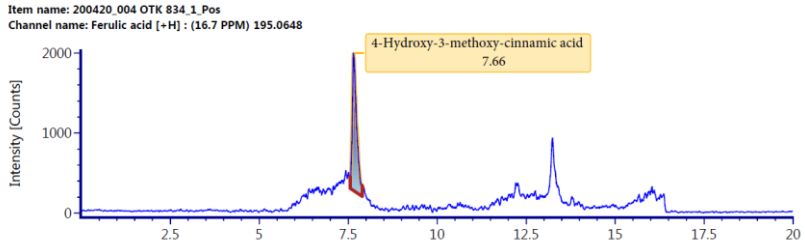

3,4-Dimethoxycinnamic acid

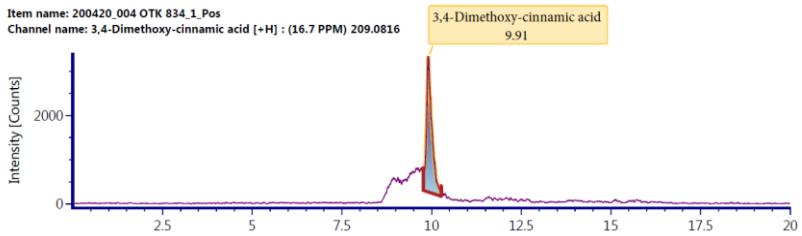

Genistin

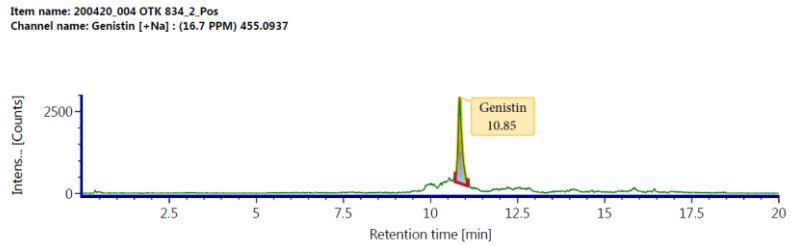

Penduletin

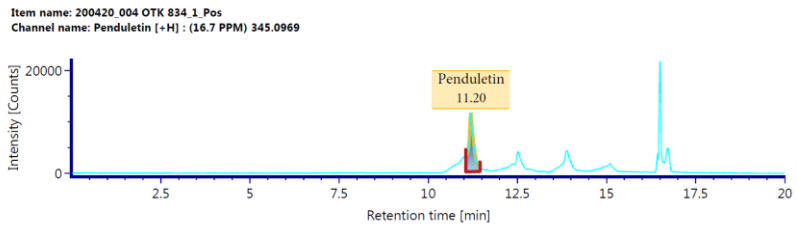

Figure S1. Eleven compounds identified in propolis by using LC-MS/MS XEVO G2XS Quadrupole time-of-flight (Q-TOF) method and identified based on the similarity percentage of retention time (Rt) and matched result parameters with criteria requirement from the database of UNIFI software.

*Criteria requirement:

1. Mass error ≤ 5 ppm
2. Isotope match MZ RMS % ≤ 11 %
3. Intensity/Response ≥ 300
4. Fragment match ≥ 1 mass fragment

Isorhamnetin

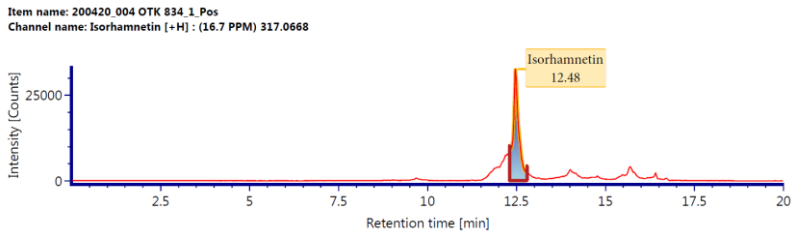

Naringenin

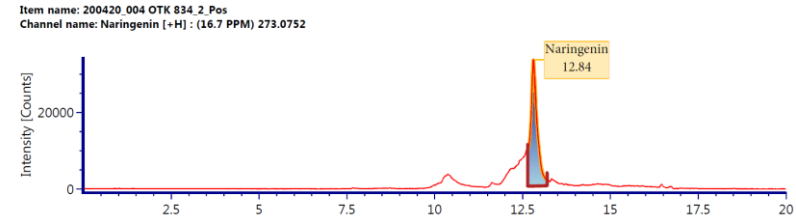

Pinostrobin

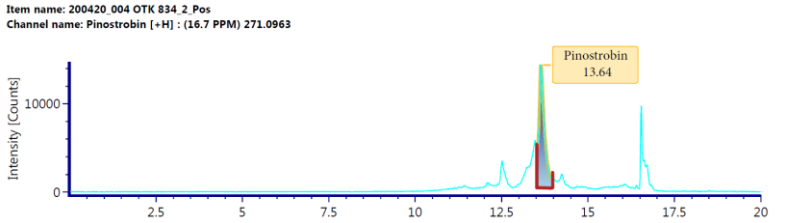

Kaempferide

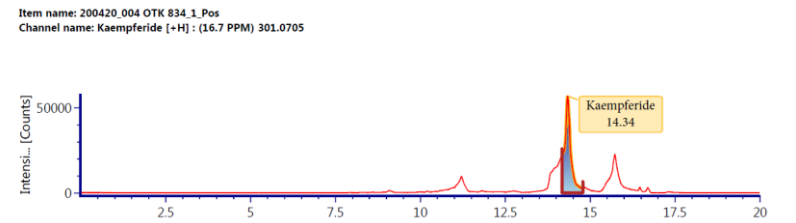

Ombuin

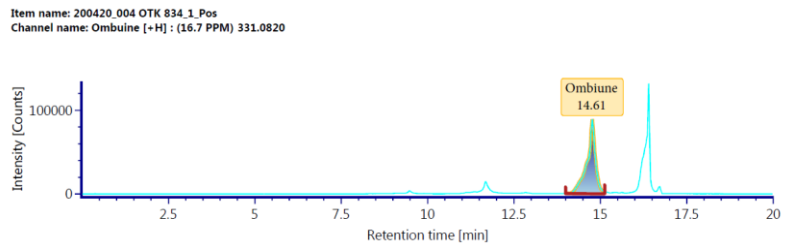

Figure S1. Eleven compounds identified in propolis by using LC-MS/MS XEVO G2XS Quadrupole time-of-flight (Q-TOF) method and identified based on the similarity percentage of retention time (Rt) and matched result parameters with criteria requirement from the database of UNIFI software (continued...)

*Criteria requirement:

1. Mass error ≤ 5 ppm
2. Isotope match MZ RMS % ≤ 11 %
3. Intensity/Response ≥ 300
4. Fragment match ≥ 1 mass fragment

Quercetin-3,3'-dimethyl ether

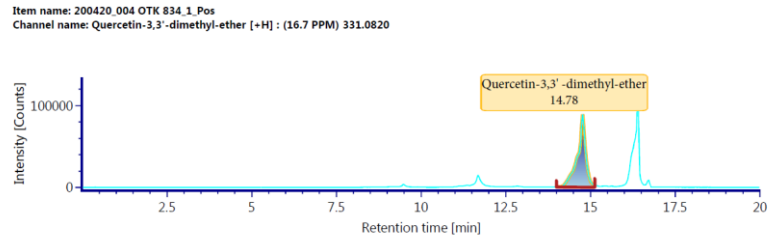

Licoflavone A

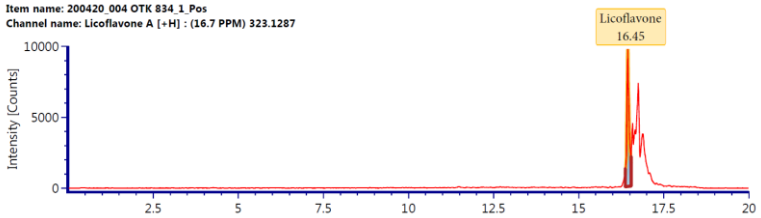

Figure S1. Eleven compounds identified in propolis by using LC-MS/MS XEVO G2XS Quadrupole time-of-flight (Q-TOF) method and identified based on the similarity percentage of retention time (Rt) and matched result parameters with criteria requirement from the database of UNIFI software (continued...)

*Criteria requirement:

1. Mass error ≤ 5 ppm
2. Isotope match MZ RMS % ≤ 11 %
3. Intensity/Response ≥ 300
4. Fragment match ≥ 1 mass fragment